

# Disc stuff

Tom Douglas<sup>1\*</sup>, Paola Caselli<sup>1</sup>

<sup>1</sup>School of Physics and Astronomy, University of Leeds, Leeds LS2 9JT, UK

In original form 2012

## ABSTRACT

Abstract here

**Key words:** circumstellar matter – infrared: stars.

## 1 INTRODUCTION

1. description of what has been done so far on the modelling and radiative transfer of disks (this includes also more evolved disks – Visser et al., Walsh et al., Aikawa et al. ..)
2. focus on the young disks (work done by Machida et al., Dapp, Basu & Kunz 2012, .. for their formation; work by Boley et al. on the physical evolution ; Ilee et al. for chemistry)
3. previous attempts to observe these young disks: (a) simulations (Cossins et al. 2010); (b) observations: Fuente et al. 2010 (AB Aur); Jorgensen & van Dishoeck ( $H_2^{18}O$  and the HDO/ $H_2O$  ratio); Pineda et al. (2012); other papers talking about "hot corinos" (Bottinelli et al. ....)

## 2 DESCRIPTION OF THE MODEL

The physical and chemical models used to simulate the emission from a young protoplanetary disc is a hybrid model created from hydrodynamical models of an infalling prestellar core and a gravitationally unstable protoplanetary disc. The prestellar core model is based upon the model of Keto & Caselli (2010). This describes an infalling pre-stellar core, with densities temperatures and velocities given by the model of the collapse of a 10 solar mass Bonnor-Ebert sphere and provides a match to line profiles seen in the pre-stellar core L1544. Some slight modification due to the addition of Oxygen lines (Keto et al 2012 in prep) have been added to this model resulting in a slight decrease in the peak infall velocity. This prestellar core model extends from 80 au out to 10,000 AU. The model is a 1D spherically symmetric model with inward motions (see figure ??).

At radii less than 80 au the physical structure is given by the hydrodynamic model described in Ilee et al. (2011), based on the work of Boley(2007), and Boley(2009). This model describes a  $0.39 M_\odot$  self-gravitating disc featuring prominent spiral arms.  $H_2$  number densities in the disc range from  $10^{10}$ - $10^{19} \text{ m}^{-3}$ , and temperatures range from

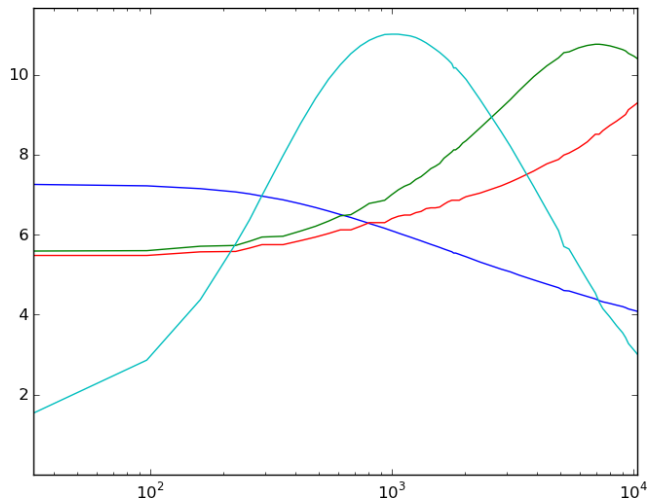


**Figure 1.** Model of the prestellar core L1544 used as the envelope in the hybrid model. Showing temperature and dust temperature (red, green) in kelvin, log number density (blue) in  $\text{cm}^{-3}$  and inward velocity $\times 100$  (cyan) in  $\text{m s}^{-1}$ . Adapted from Keto & Caselli (2010)

30-400 K (figure 2). The dust and gas temperatures in the disc are assumed to be in equilibrium. The model is sampled over a regular grid of size  $256 \times 256 \times 64$  with spatial resolution of 0.5 au in x, y and z. The majority of the mass lies in the mid-plane of the disc. For the models using a smoothed disc the same physical and chemical model is used but with the temperature, density and abundance averaged in  $\phi$ . The gas/dust mass ratio was assumed to be 1/100 throughout both sections model and the opacities were given by the model of dust grains with thick icy mantles and  $10^6$  yr coagulation from Ossenkopf and Henning (1994)

Chemical abundances in the disc were taken from Ilee et. al (2011) which followed the changes of chemical abundances of trace particles moving through the disc as it evolved. The abundances of 125 species related by 1334 reactions were followed through the time evolution of

\* E-mail: pytd@leeds.ac.uk

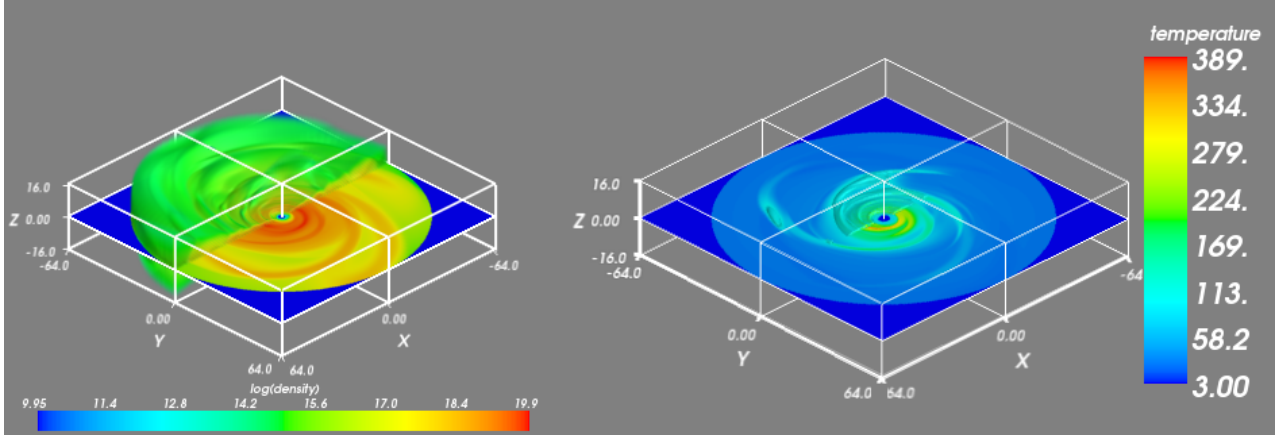


**Figure 2.** Left: A 3D plot of log number density ( $\text{m}^{-3}$ ) showing the spiral structure in the  $xy$  plane and scale height of the disc. Right: The 3D temperature structure of the disc; regions cooler than 40 degrees are not shown in 3D, demonstrating the narrow central region containing hot material.

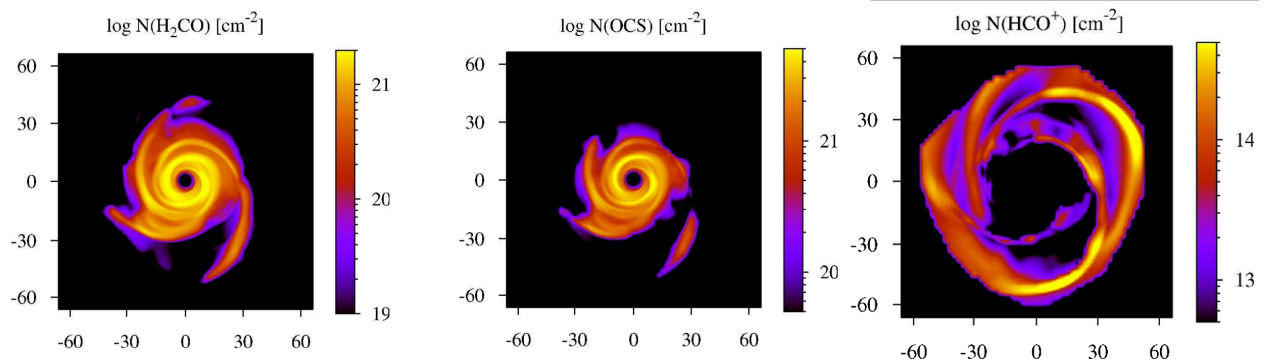


**Figure 3.** Column densities of  $\text{H}_2\text{CO}$ , OCS and  $\text{HCO}^+$  used in the disc model. Figure adapted from Ilee et al. (2011)

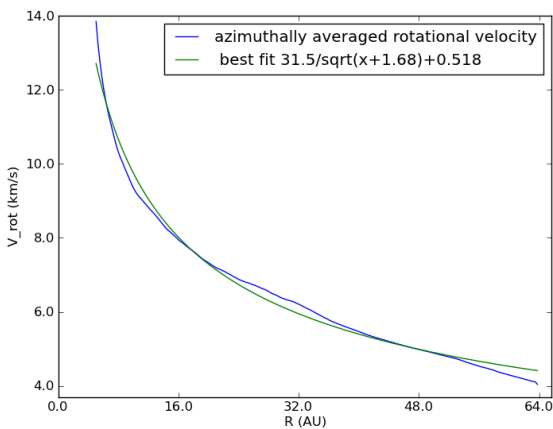


**Figure 4.** Azimuthally averaged rotational velocity in the disc mid-plane with best fit curve

the disc. These abundances were interpolated onto a 51<sup>3</sup> grid covering the disc with cells of size  $2.2 \times 2.2 \times 0.22$  au. Abundances in the envelope model were as follows:

$\text{HCO}^+$ : As the  $\text{H}_2\text{O}$  profile from Caselli et al. (2012, submitted) scaled so that the maximum abundance is  $10^{-8}$   
 $\text{HNO}$ : Constant abundance of  $5 \times 10^{-11}$   
 $\text{HCS}^+$ : Constant abundance of  $10^{-11}$   
 $\text{OCS}$ : Constant abundance of  $10^{-9}$   
 $\text{H}_2\text{CO}$ :  $1.5 \times 10^{-9}$  decreased by a factor of 40 at radii less than 8250au (Young et al 2004)  
 $\text{CS}$ :  $3 \times 10^{-9}$  decreased by a factor of 10,000 at radii less than 6700au (Tafalla, Santiago-garcia and myers 2006)  
 $\text{CO}$ : As the  $\text{H}_2\text{O}$  profile from Caselli (2012, submitted) scaled so that the maximum abundance is CO maximum \*\*\*which is....\*\*\*

The radiative transfer program used, LIME (Brinch 2011), calculates line intensities based on a weighted sample of randomly chosen points in a continuous 3d model. The method of selecting these points is given in the gridding section. At each of these points the density of the main collision partner (in this case  $\text{H}_2$ ), gas and dust temperatures, velocity, molecular abundances and turbulent velocity and taken from the model. These points are then smoothed by Lloyds algorithm (Lloyd 1982) in order to minimise the variation in distance between points whilst keeping the same underlying distribution. These points are then connected by Delaunay triangulation and it is down these paths that photons are restricted to propagating (figures 2). The levels

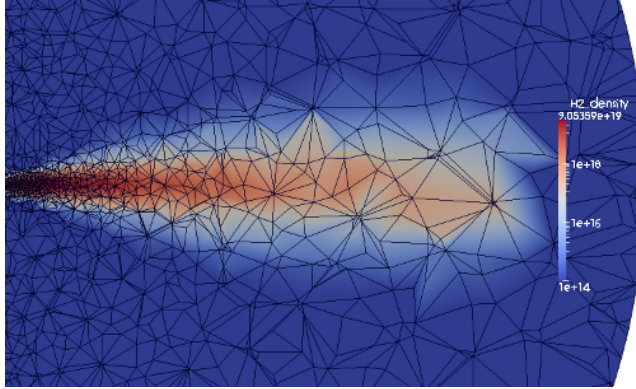


**Figure 5.** A plot of the points selected by the gridding process and the paths down which photons can propagate overlaid on a smoothed density model. The points are more concentrated at small radii and in the densest regions.

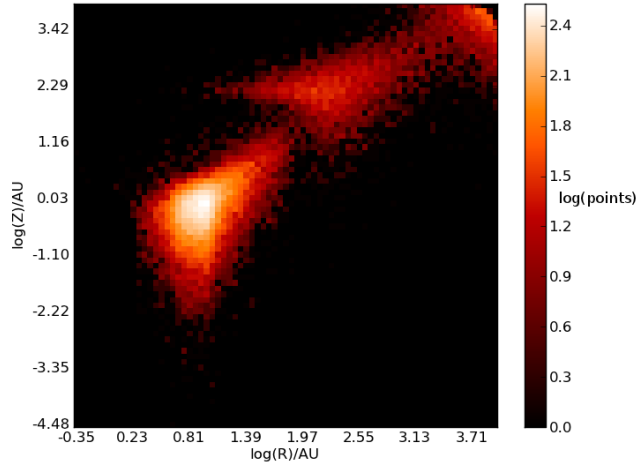


**Figure 6.** A histogram of the point distribution throughout the model.

of molecules in question are then calculated at each of these points from collisional and radiative (de)excitation and the local radiation field is calculated. This is repeated 20 times with the populations of each level converging towards a single value.

In order to construct the grid, points are randomly selected from the volume being simulated then compared against a reference point. Grid points are selected at random in cylindrical co-ordinates, linearly spaced in  $z$  and  $\phi$  and logarithmically spaced in  $r$ . For each point to be selected a random number  $\alpha$  is drawn from the semi-open set  $[0, 1)$  as a threshold. After selection of random co-ordinates the Hydrogen density and molecular density at the point ( $n$  and  $m$ ) are compared against the densities of a reference point on the inner edge of the disc ( $n_0$  and  $m_0$ ). If  $\alpha < \left(\frac{n}{n_0}\right)^{0.3}$  or  $\alpha < \left(\frac{m}{m_0}\right)^{0.3}$  then the point is selected for use, if not then another  $r, \phi, z$  co-ordinate is selected. The weighting function and gridding functions were selected empirically to sample both the all scales while ensuring the majority

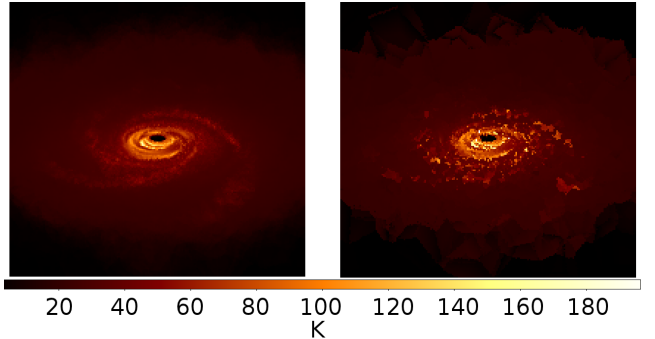


**Figure 7.** A plot showing the difference between a single LIME continuum image at 300 GHz (right) and the average of ten such images from different runs of the same model in LIME (left).

of the points went into the inner disc which is the region of interest. 20% of these points are forced to be at radii greater than  $\sqrt{R_{min}R_{max}}$  (where  $R_{min}$  and  $R_{max}$  are the inner and outer radius of the model) in order to stop too many of the selected points clustering in the high density disc and leaving the envelope undersampled. In addition to this method of selection 5% of the points are linearly distributed in  $x$ ,  $y$  and  $z$  with no bias with regards to density or abundance. This provides a minimum level of sampling for the large low density regions in the outer parts of the simulated volume. See figure 2 for example of the points distribution in  $r$ ,  $z$ .

### 3 MODEL RESULTS

The results of these simulations for the molecules OCS,  $\text{HCO}^+$ ,  $\text{H}_2\text{CO}$  and isotopologues of CO are shown here, other molecules simulated but not shown include HCN, HNC, HNO, HCS<sup>+</sup> and CS. For the purpose of simulating observations the model was placed at roughly the distance of nearby low-mass star forming regions (100 pc) and is inclined 30° to edge on. From these observations integrated intensity, intensity weighted velocity and position velocity diagrams through the centre of the model were created. The simulations done are focused upon frequencies within ALMA band 7, selected to give the best trade off between resolution and sensitivity for early ALMA science. (Note the moment 1 and 0 maps were created by integrating between -12.5 to -0.5  $\text{km s}^{-1}$  and +0.5 to +12.5  $\text{km s}^{-1}$  to avoid being dominated by the contribution from the envelope, this can be seen in some PV diagrams as the strong absorption feature at all positions around zero velocity, moment 1 maps are shown with a cutoff of 1/1000 of the peak emission/absorption value)

Figures 6, 7 and 8 show synthetic images of the CO J=3-2 line at 345.8 GHz. As the upper level for this line is at 33 K above the ground state this transition should be excited through out disc given the large and uniform nature of the abundance of CO in the disc this line will be optically thick and this is only mapping the outer regions of the disc. In common with most transitions simulated,

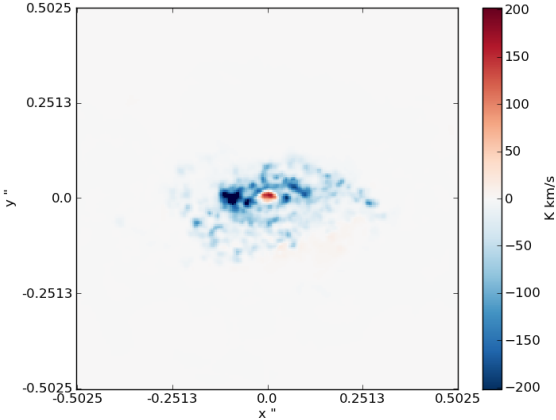


**Figure 8.** CO J=3-2 Continuum subtracted mom0

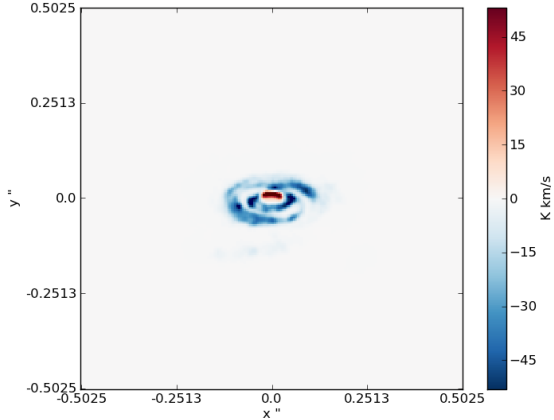


**Figure 11.** OCS 28-27 Continuum subtracted mom0

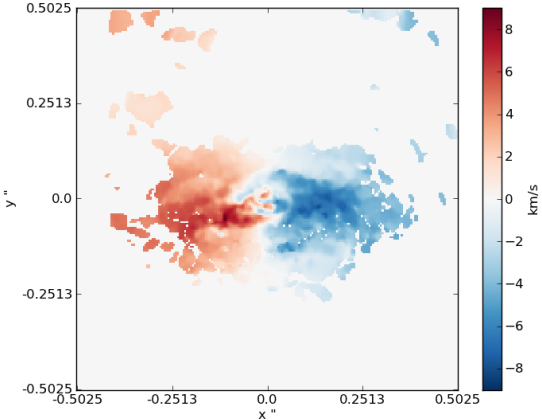


**Figure 9.** CO J=3-2 moment 1 map

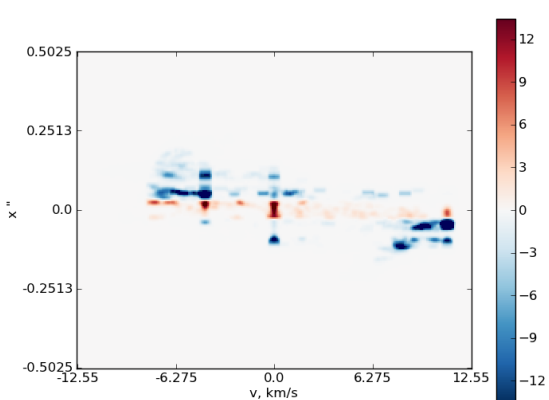


**Figure 12.** OCS 28-27 PV through centre

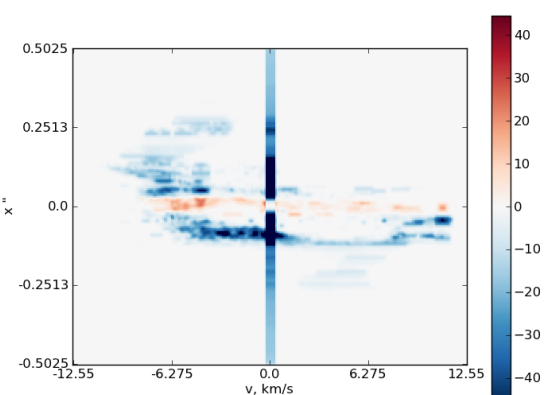


**Figure 10.** CO J=3-2 PV through  $y=0''$

the line is seen almost exclusively in absorption against the disc continuum. The region of emission in the centre is where there is no continuum background to be absorbed. Some indications of spiral structure can be seen but are indistinct. \*\*\*not sure how useful these are, might be worth cutting them?\*\*\*

After looking at a variety of lines which could be observed of ALMA band 6 or 7 (211-275 GHz and 275-373 GHz) we found that the OCS lines in alma band 7 (22-21 through 30-29) with upper energy levels between 161 and 271 K above the ground state provide a way to trace hot shocked gas in spiral arms without resolving structure. Figures 3 & 3 show the integrated intensity of the OCS J=28-27 line in the model described previously and one where the disc section of the model is an axis-symmetric model created by taking the azimuthal average of density, temperature and molecular abundance. The order of magnitude difference in the line intensity provides a method to detect hot dense gas without being able to resolve the spiral structure spatially.

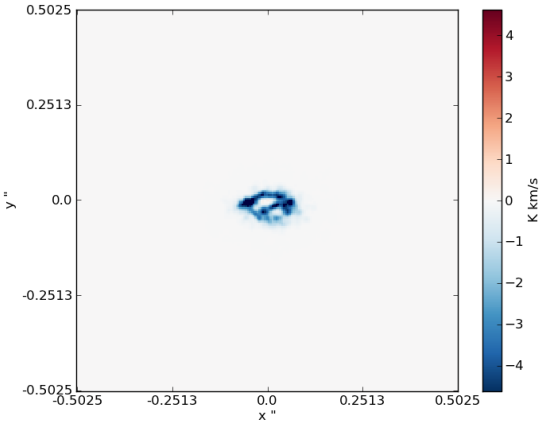


**Figure 13.** SmoothedOCS 28-27 Continuum subtracted mom0

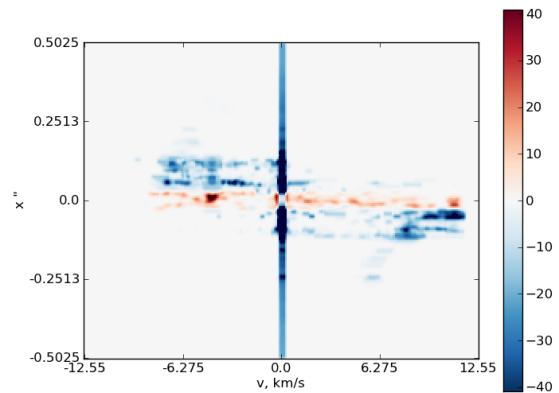


**Figure 16.** H<sub>2</sub>CO 4 0 4 - 3 0 3 PV through centre

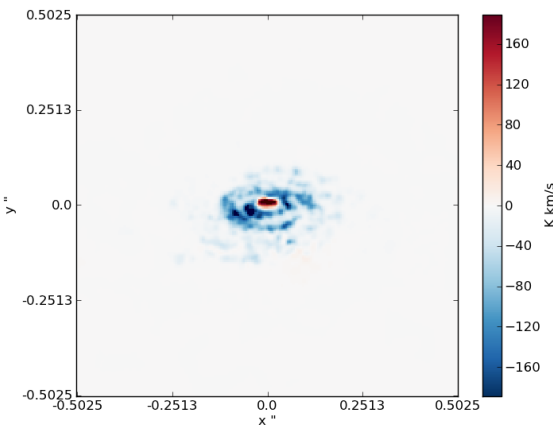


**Figure 14.** H<sub>2</sub>CO 4 0 4 - 3 0 3 Continuum subtracted mom0

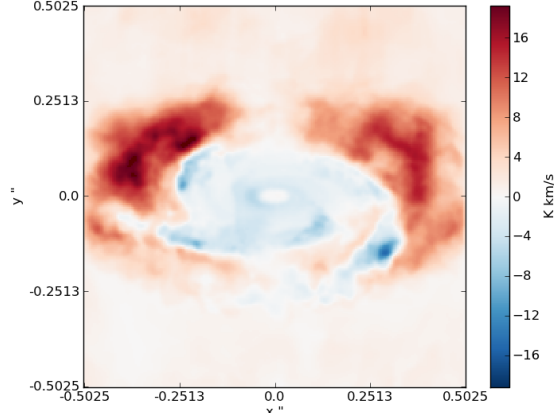


**Figure 17.** HCO<sup>+</sup> 1-0 Continuum subtracted mom0

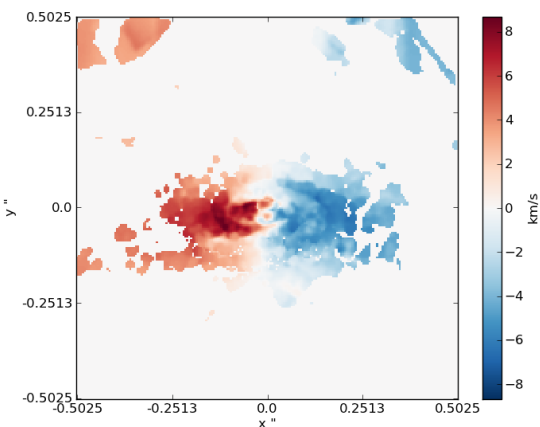


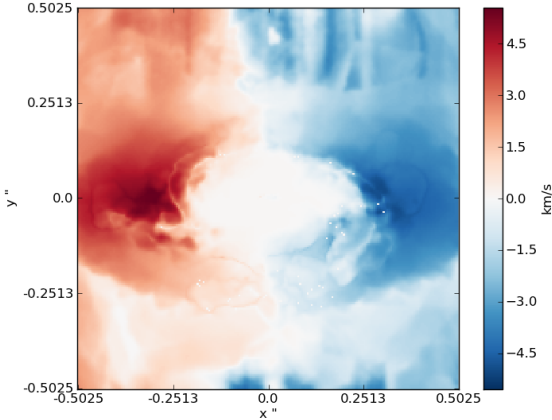
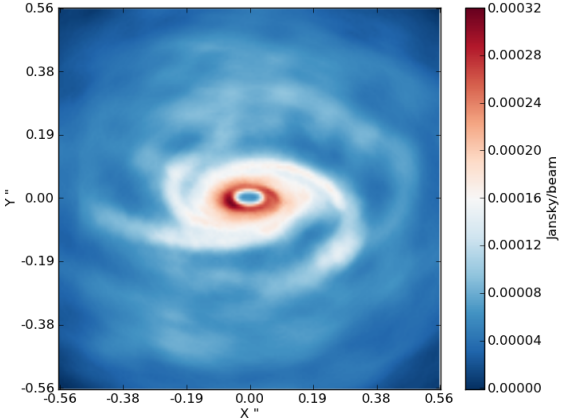
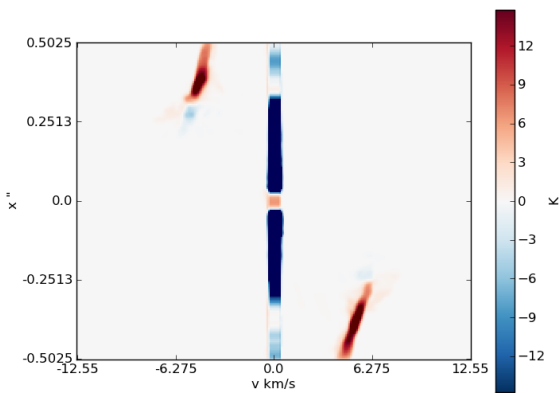
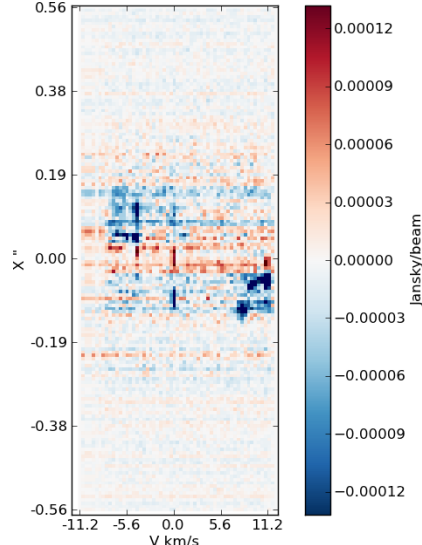
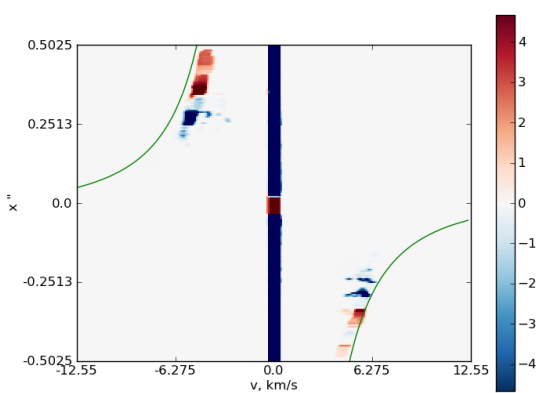
**Figure 15.** H<sub>2</sub>CO 4 0 4 - 3 0 3 PV through centre

More complex molecules such as H<sub>2</sub>CO with many closely spaced spectral lines can be used to gain an estimate on the temperature of a region.

(figure of temperature as a function of line ratio for 2 sets of formaldehyde lines and map of derived temperature, talk to P about this. This doesn't seem doable with the lines around 1mm for alma)

Some molecules such as HCO<sup>+</sup> trace only the outer regions of the disc (Ilee 2011) and so can be used to look at the extended velocity and physical structure. In these colder less dense regions we see the molecular lines in emission rather than absorption. Figure 3 shows the rotation curve of the model as shown in figure 2 against the HCO<sup>+</sup> J=3-2 line emission. It is clear that from observations such as these the rotation curve of a disc could be reconstructed.

In all the simulations except HCO<sup>+</sup> we see molecular lines in absorption throughout the majority of the disc and in some cases a small amount of emission towards the centre, where the inclination of the disc allows us the view

**Figure 18.**  $\text{HCO}^+$  1-0 mom1map**Figure 21.** continuum emission at 337GHz simulated for ALMA most extended configuration**Figure 19.**  $\text{HCO}^+$  1-0 pv through centre**Figure 22.** OCS 28-29 pv diagram simulated for ALMA most extended configuration**Figure 20.**  $\text{HCO}^+$  3-2 PV through centre with rotation curve from figure 2 \*\*\* should the velocities in this be reduced by  $\cos(30)$  as we're not in the plane of rotation? \*\*\*

the low density but moderate temperature region inside the inner edge of the spiral structures without any high temperature and density material behind it.

#### 4 ALMA PREDICTIONS

#### 5 DISCUSSION

In this paper we have performed radiative transfer simulations of a hybrid model comprising a  $0.4 M_\odot$  self gravitating disc with radius  $64 \text{ AU}$  showing spiral density waves, surrounded by an envelope simulated as a collapsing  $10 M_\odot$  BE-sphere. CASA simulations show that at a distance of  $100 \text{ pc}$  both spatial resolution of the spirals in such a disc and extraction of kinematic and temperature from molecular lines are possible in ALMA band 7. Our simulations show that many molecular species are predominantly

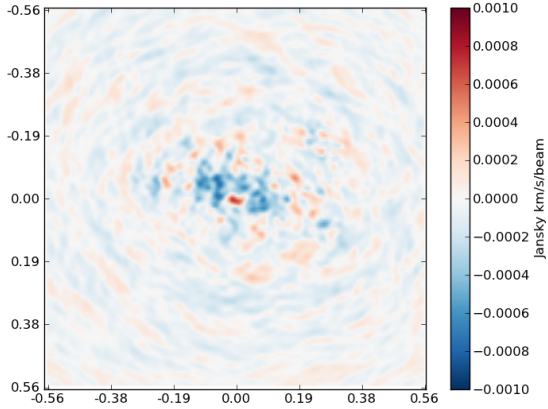


**Figure 23.** OCS 28-29 integrated intensity simulated for ALMA most extended configuration

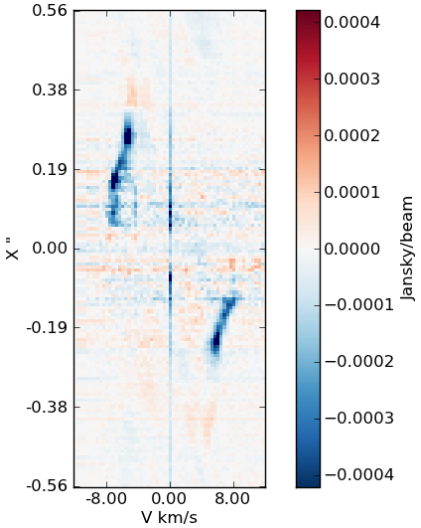


**Figure 24.** C17O 3-2 30 deg PV through centre simulated for ALMA most extended configuration

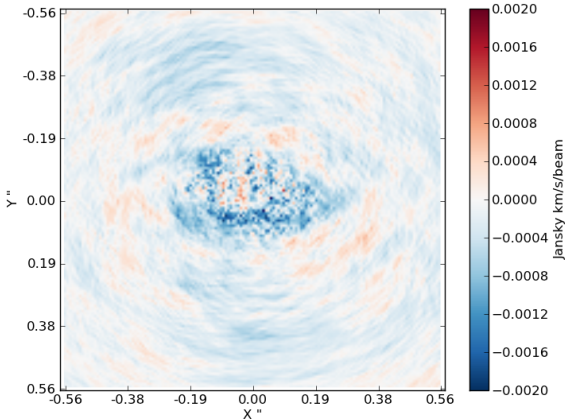


**Figure 25.** C17O 3-2 30 deg integrated intensity simulated for ALMA most extended configuration

seen in absorption towards the centre of self-gravitating protoplanetary discs. The quiescent nature of the envelope around such discs only obscures them within  $\pm 0.5 \text{ km s}^{-1}$ . Hot, shocked gas can be detected in such a disc without resolving it by observing OCS transitions between 26-27 to 30-29.

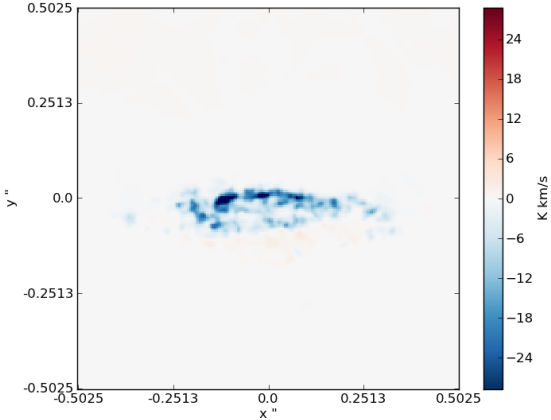
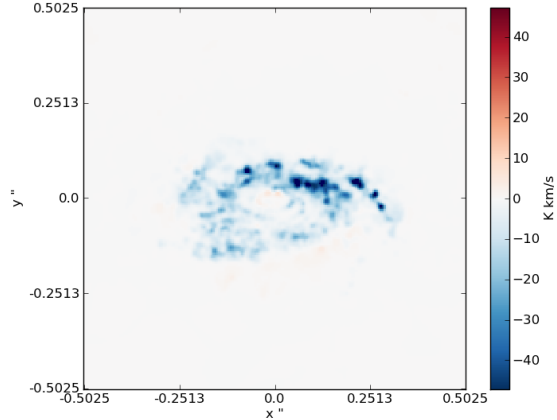
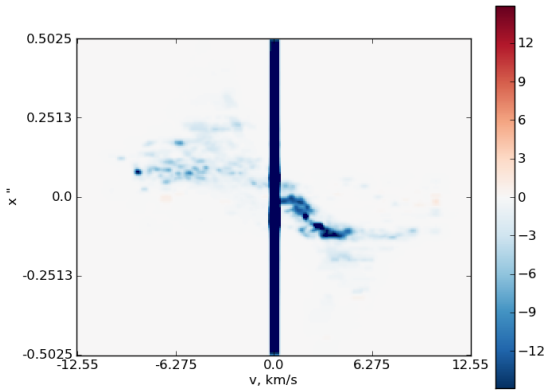
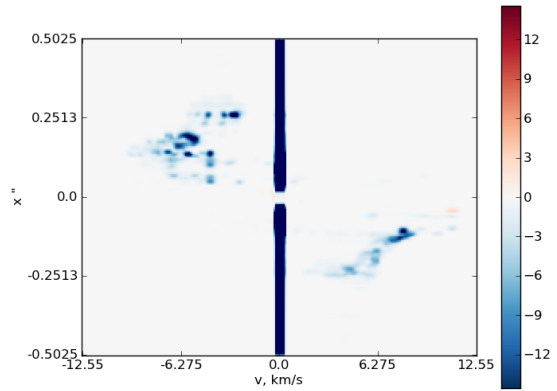
One assumption made in this model is that the gas and dust are in thermal equilibrium. If they are not and the dust is significantly cooler than the gas then transitions may not show up in absorption.

The mass of the disc used ( $0.4 M_{\odot}$ ) is on the high end for early discs (citations for estimate of early class 1 disc masses).

In the model spirals shock heat the mid-plane layer and the colder more diffuse gas absorbs the continuum from it, this results in molecular lines being seen in absorption whenever lines of sight pass through the cold diffuse gas at larger heights on to the hot dense midplane of the disc. Rotation curves can be gathered from these observations even with spiral structure

## ACKNOWLEDGEMENTS

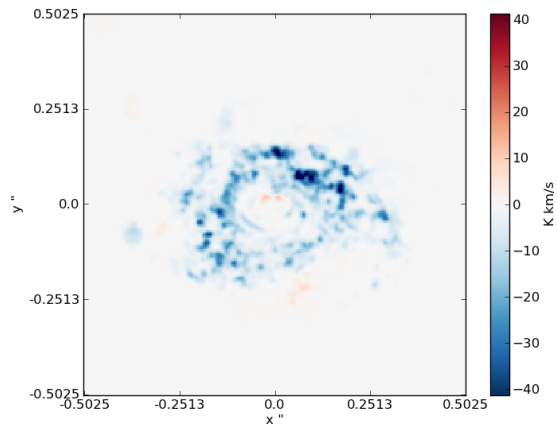
stuff here

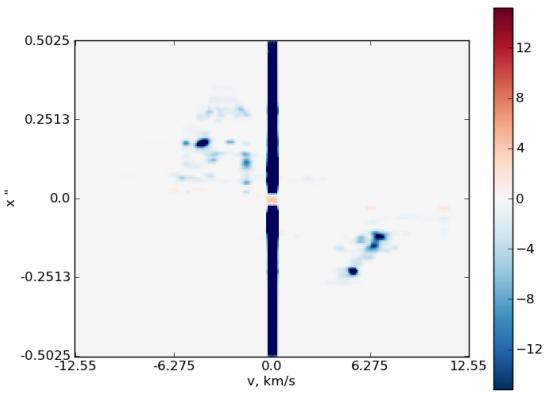
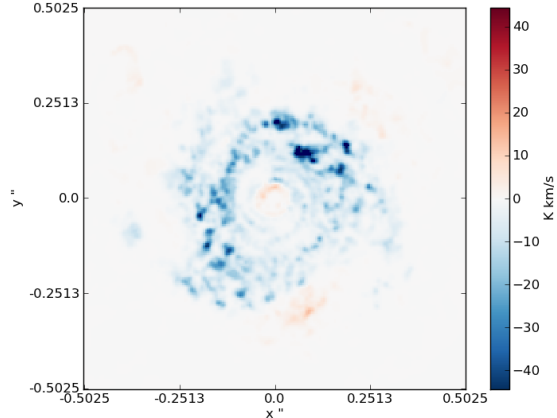
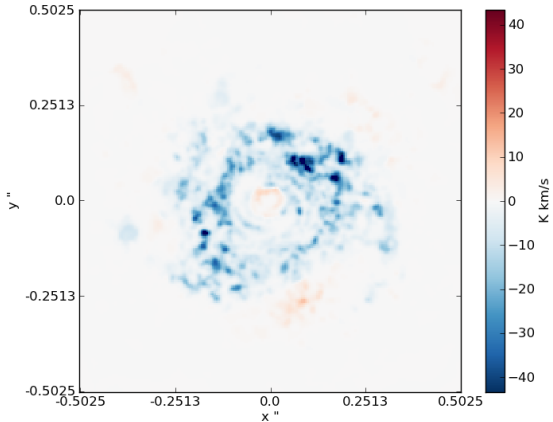
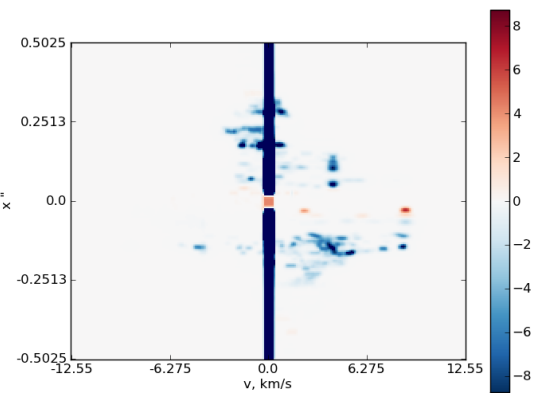
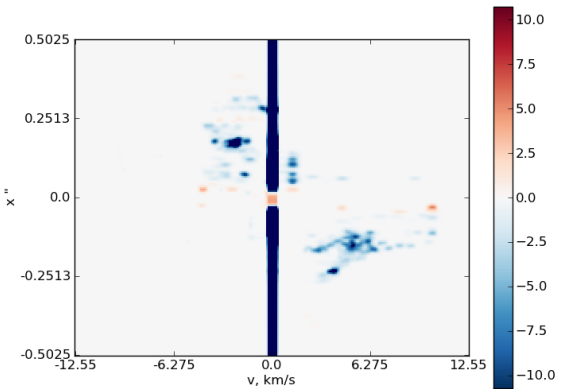
**Figure A1.** C18O 3-2 15 deg Continuum subtracted mom0**Figure A3.** C18O 3-2 30 deg Continuum subtracted mom0**Figure A2.** C18O 3-2 PV 15 deg through centre**Figure A4.** C18O 3-2 30 deg PV through centre

## APPENDIX A: OTHER INCLINATIONS

Figures showing different inclinations

This paper has been typeset from a T<sub>E</sub>X/ L<sup>A</sup>T<sub>E</sub>X file prepared by the author.

**Figure A5.** C18O 3-2 45 deg Continuum subtracted mom0

**Figure A6.** C18O 3-2 45 deg PV through centre**Figure A9.** C18O 3-2 75 deg Continuum subtracted mom0**Figure A7.** C18O 3-2 60 deg Continuum subtracted mom0**Figure A10.** C18O 3-2 75 deg PV through centre**Figure A8.** C18O 3-2 60 deg PV through centre